Journal of Dental Sciences 20 (2025) 1824–1831

Available online at www.sciencedirect.com

ScienceDirect

journal homepage: www.e-jds.com

Original Article

Dynamic contrast-enhanced magnetic resonance imaging of masticatory muscles in patients with idiopathic condylar resorption

Yu-Chen Wang [a], Hsiao-Chiao Yeh [a], Yunn-Jy Chen [b], Tiffany Ting-Fang Shih [a,c*]

[a] *Department of Medical Imaging, National Taiwan University Hospital, Taipei, Taiwan*
[b] *Department of Dentistry, School of Dentistry, National Taiwan University and Hospital, Taipei, Taiwan*
[c] *Department of Radiology, National Taiwan University College of Medicine, Taipei, Taiwan*

Received 31 March 2025; Final revision received 27 April 2025
Available online 14 May 2025

KEYWORDS
Dynamic contrast enhanced magnetic resonance imaging;
Idiopathic condylar resorption;
Mandibular condyle;
Masticatory muscles;
Temporomandibular joint disorders

Abstract *Background/purpose:* Idiopathic condylar resorption (ICR), a subset of temporomandibular disorders (TMDs), presents an unclear relationship between structural changes in the mandibular condyle and alterations in masticatory muscle perfusion. This study aimed to investigate the correlation between mandibular condyle structural changes and masticatory muscle perfusion in patients with ICR using dynamic contrast-enhanced (DCE) magnetic resonance imaging (MRI).
Materials and methods: From July 2018 to August 2022, patients with ICR from hospital-based TMD clinics underwent conventional and DCE MRI examinations. The patients were categorized on the basis of the degree of temporomandibular joint (TMJ) condylar resorption into grade 0 (normal), grade 1 (mild to moderate), and grade 2 (severe). DCE MRI parameters of masticatory muscles responsible for mouth closing (masseter [MA] and medial pterygoid [MP]) and opening (lateral pterygoid [LP]) were examined.
Results: Among 79 patients (158 TMJs), 41 % were assigned to the grade 0 group, 29 % were assigned to the grade 1 group, and 30 % were assigned to the grade 2 group. No significant differences in demographic or physical parameters were observed between the groups. In cases of severe condylar resorption (grade 2), the LP muscle exhibited a marked increase in plasma volume; none of the other muscles exhibited significant variations in plasma volume.
Conclusion: Increased plasma volume perfusion of the LP muscle is correlated with the severity of TMJ condylar resorption, indicating a specific correlation between muscle function and ICR severity. DCE MRI is useful for exploring muscular adaptation in patients with ICR and TMDs.

* Corresponding author. Department of Radiology and Medical Imaging, College of Medicine and Hospital, National Taiwan University, No. 7, Chung-Shan South Road, Taipei 100, Taiwan.
E-mail address: ttfshih@ntu.edu.tw (T.T.-F. Shih).

https://doi.org/10.1016/j.jds.2025.04.031

Introduction

Idiopathic condylar resorption (ICR) is a progressive disorder of the temporomandibular joint (TMJ), characterized by the loss of condylar height and structural deformation.[1,2] This condition predominantly affects female individuals during their developmental stage, particularly around puberty, and is associated with facial pain, malocclusion, and aesthetic changes.[3–5] Diagnosing ICR is a complex process that requires the exclusion of other mandibular diseases and the differentiation of ICR from various systemic, local, and developmental conditions.[6,7]

In clinical settings, diagnosing ICR and other temporomandibular disorders (TMDs) relies on a combination of patient history, clinical findings, and radiological assessments. Although traditional radiography can provide initial insights, its usefulness is limited because it only has the capability of taking two-dimensional images. Consequently, more advanced imaging techniques, such as ultrasonography, cone beam computed tomography (CBCT), and magnetic resonance imaging (MRI), have been developed. Although CBCT has improved the understanding of TMJ bone pathology,[8] MRI remains the modality of choice for examining the soft tissue components of TMJs.[9,10] Dynamic contrast-enhanced (DCE) MRI represents a major advancement that offers quantitative evaluations of perfusion patterns in soft tissues.

Previous studies have indicated the value of DCE MRI in evaluating synovitis and retrodiscal tissues in TMJs.[11–14] However, a major gap remains in understanding how changes in masticatory muscles correlate with morphological alterations in the condylar structure of patients with ICR. In this study, to address this gap, we used DCE MRI to examine the correlations between condylar changes and alterations in the perfusion of masticatory muscles in patients with ICR.

Materials and methods

Study design

This prospective cross-sectional study was conducted from July 2018 to August 2022 and was approved by the Institutional Review Board of our hospital (IRB No. 201712100RINB). Written informed consent was obtained from all participants prior to enrollment. Patients were referred by a specialist in TMJ disorders (Y.J.C.) from hospital-based TMJ disorder clinics for MRI evaluation.

The inclusion criteria were as follows: (1) age between 15 and 55 years; (2) both male and female patients; (3) radiographic evidence of TMJ condylar contour changes observed during orthodontic assessment; (4) presence of anterior open bite or mandibular retrusion; (5) severe limitation in maximal mouth opening; or (6) TMJ pain unresponsive to conservative treatments. Exclusion criteria included: (1) age above 55 years, to minimize the potential confounding effects of age-related TMJ osteoarthritic changes; (2) history of orthognathic surgery; and (3) prior head and neck plastic surgery.

Data acquisition

Imaging was performed using a 1.5-T MRI scanner (MAGNETOM Aera; Siemens Healthineers, Erlangen, Germany) equipped with a 20-channel head/neck coil. Images of closed-mouth neutral positions were captured, with the sagittal view oriented perpendicular to the condylar long axis. The following MRI protocol was implemented: (1) sagittal T1–weighted images with defined parameters (repetition time [TR] = 542 ms, echo time [TE] = 10 ms, flip angle = 150°, slice thickness = 3 mm, field of view [FOV] = 12 × 12 cm), (2) sagittal gradient echo T2–weighted images with set parameters (TR = 479 ms, TE = 23 ms, flip angle = 35°, slice thickness = 2 mm, FOV = 12 × 12 cm), and (3) DCE MRI with gadobutrol (Gadovist; Bayer AG, Barmen, Germany) administered at a rate of 2 mL/s at 0.1 mmol/kg body weight. DCE MRI images were captured as T1-weighted oblique coronal images of bilateral TMJs in the FOV with the following parameters: TR/TE = 3.1/1.2 ms, flip angle = 12°, slice thickness = 4 mm, FOV = 24 × 24 cm. Temporal resolution was set at 2.4 s (0.13 s/section, with 18 consecutive sections for 2.4 s). The first five scans (12 s) were set as the baseline for precontrast, and gadobutrol was administered from the 6th to the 55th scan (13–144 s) for postcontrast imaging, with a temporal resolution of 2.4 s.

Imaging analysis

In accordance with previous studies, mandibular condylar deformities were graded 0 (normal), grade 1 (mild-to-moderate), and grade 2 (severe) resorption.[15,16] These grading evaluations were conducted by two radiologists, namely Y.C.W. and T.F.S., who had 7 and 32 years of experience, respectively, in musculoskeletal imaging. DCE MRI imaging data were analyzed using MIStar (Apollo Medical Imaging Technology, Melbourne, Australia). Arterial input function was determined by placing a region of interest (ROI) on the right carotid artery bifurcation. Manual demarcations were made on DCE MRI image slices with an appropriate cross-sectional area for three pairs of masticatory muscles, namely the masseter (MA), medial pterygoid (MP), and lateral pterygoid (LP), with care taken to exclude non-muscular structures and visible vessels. To determine interobserver variability, two radiologists (Y.C.W. and H.C.Y.) with independently drew the ROIs, and their measurements were compared.

Two-compartment Tofts model analysis was conducted to facilitate the calculation of pharmacokinetic

parameters.[17] Quantitative parameters such as the volume transfer constant between blood plasma and the extravascular extracellular space (EES, K_{trans} in min^{-1}), the rate constant between the EES and blood plasma (k_{ep} in min^{-1}), the volume of the EES per unit volume of tissue (v_e in %), and blood plasma per unit volume of tissue (v_p %) were automatically derived.

Statistical analysis

Interobserver variability was evaluated using a two-way mixed-effects model, with intraclass correlation coefficients (ICC) and 95 % confidence intervals calculated. The chi-square test was conducted to determine differences in sex proportions and TMJ laterality between different condylar morphology groups. The Kruskal–Wallis test was used to examine age, body mass index (BMI), and median differences in all DCE MRI biomarkers across various osseous condylar resorption groups. Pairwise comparisons within the Kruskal–Wallis test were adjusted using Bonferroni's correction. Statistical significance was established at P- value < 0.05 for both the Kruskal–Wallis and chi-square tests. All statistical analyses were conducted using IBM SPSS Statistics version 26.0 for Windows (released in 2019; IBM, Armonk, NY, USA).

Results

Study participants

A total of 85 patients were initially enrolled in the study. One patient was excluded due to technical failure during the DCE-MRI acquisition, and five patients aged over 55 years were excluded according to the predefined criteria. A flowchart summarizing the participant selection process is presented in Fig. 1.

Ultimately, 79 patients (158 temporomandibular joints, TMJs) met the eligibility criteria and were included in the imaging analysis. Based on MRI-assessed condylar morphology, the TMJs were categorized into three groups: grade 0 (normal; 64 TMJs, 41 %), grade 1 (mild to moderate resorption; 46 TMJs, 29 %), and grade 2 (severe resorption; 48 TMJs, 30 %) (Fig. 2).

Patient demographic characteristics, including age, sex, BMI, and TMJ laterality, are summarized in Table 1. No

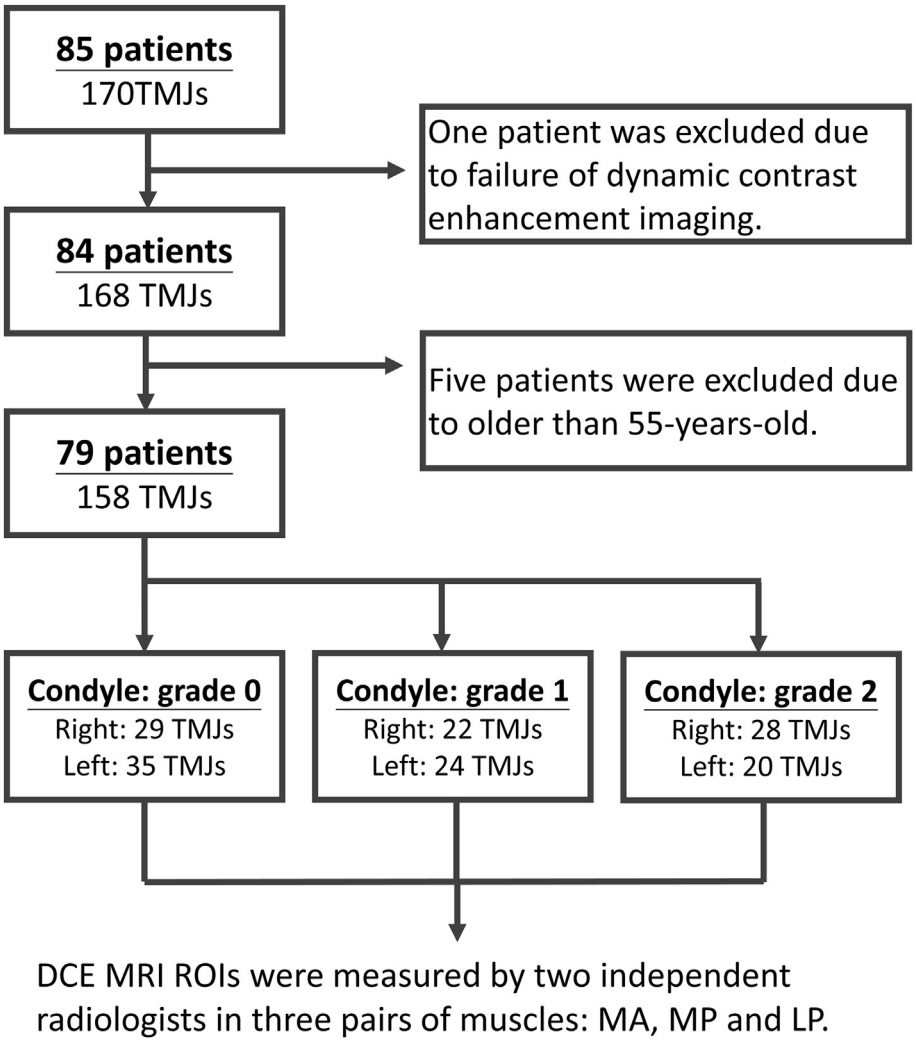

Figure 1 Patient selection criteria.

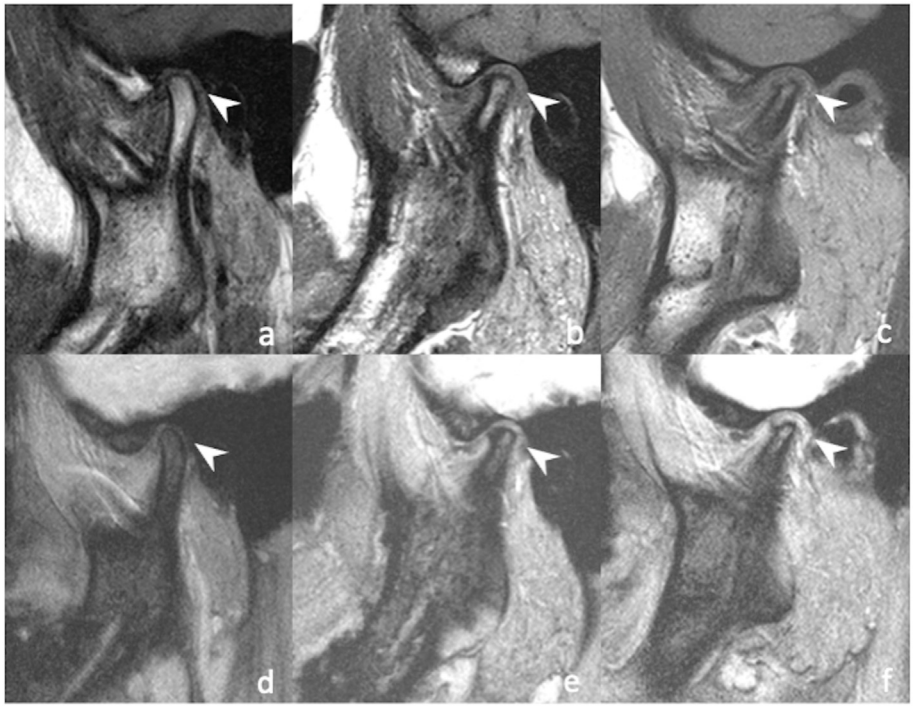

Figure 2 Grading of osseous deformities in mandibular condyle on sagittal MRI images. Upper series (**a**–**c**) depicts sagittal T1–weighted MRI scans, and lower series (**d**–**f**) depicts gradient echo T2–weighted MRI scans. Osseous changes in mandibular condyle are categorized as grade 0 for normal (**a, d**), grade 1 for mild-to-moderate (**b, e**), and grade 2 for severe (**c, f**).

Table 1 Patient demographic characteristics and TMJ laterality in each severity group.

	Condyle grade 0		Condyle grade 1		Condyle grade 2		*P*-value
	Median/N (%)	(Q1, Q3)	Median/N (%)	(Q1, Q3)	Median/N (%)	(Q1, Q3)	
TMJ numbers	64 (41 %)		46 (29 %)		48 (30 %)		
TMJ side: left/right	35/29		24/22		20/28		0.371
Age, year-old	29.3	(24.4, 40.5)	31.2	(25.3, 39.2)	32.4	(24.7, 36.7)	0.695
Sex							
Men-no.	7 (10.9 %)		6 (13.0 %)		7 (14.6 %)		0.913
Women-no.	57 (89.1 %)		40 (87.0 %)		41 (85.4 %)		
BMI	20.4	(18.1, 23.1)	19.6	(18.5, 21.2)	19.3	(17.9, 21.1)	0.265

BMI: body mass index.
Side and sex = chi-squared test.
Age and BMI: Kruskal–Wallis test.

statistically significant differences were found in age, BMI, or sex distribution among the three condyle groups.

Interobserver variability in DCE MRI analysis

Fig. 3 illustrates the selection of representative images and three ROIs of masticatory muscles. High interobserver variability (with an ICC coefficient of >0.9) was observed for DCE parameters in all pairs of masticatory muscles (Table 2).

Quantitative analysis of DCE MRI biomarkers

Table 3 presents the medians of quantitative DCE MRI biomarkers calculated using the Tofts model. The Kruskal–Wallis test revealed a significant difference in plasma volume (v_p) in the LP muscle between groups ($P = 0.032$). Pairwise comparisons adjusted with Bonferroni's correction (Fig. 4) revealed that the median plasma volume for condyle grade 2 ($v_p = 58.2$) was significantly higher ($P = 0.031$) than that for condyle grade 0 ($v_p = 26.1$). No significant differences in K_{trans}, k_{ep}, or v_e were observed between the medians of different quantitative DCE MRI biomarkers in the MA and MP muscles.

Discussion

In this study, we discovered a significant increase in the plasma volume value (v_p) of the LP muscle in TMJs with severe condylar resorption (grade 2) in comparison with

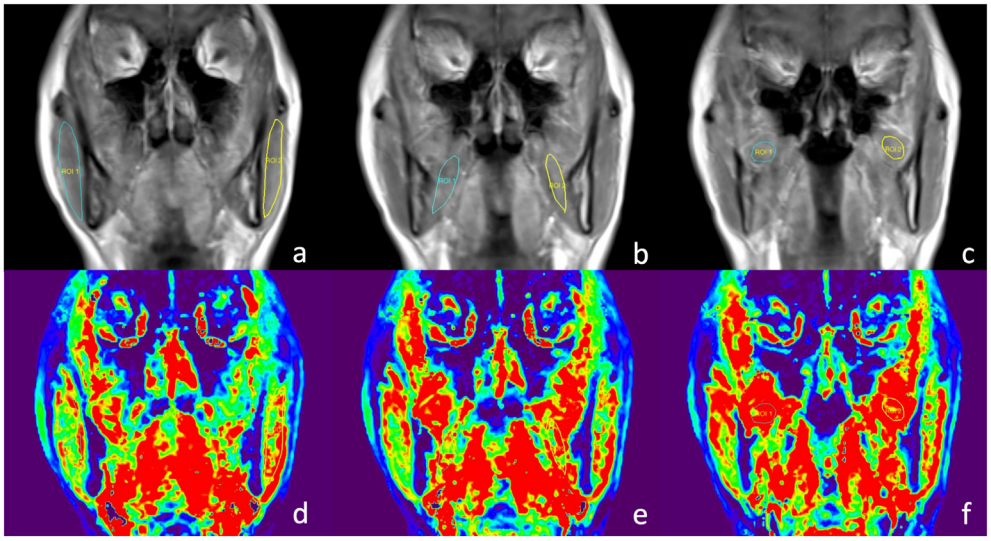

Figure 3 Selection of images and manual tracing of ROIs in three masticatory muscle pairs on DCE MRI images. Upper series (**a**—**c**) depicts coronal T1—weighted MRI scans after contrast administration, and lower series (**d**—**f**) depicts corresponding color-coded DCE MRI images (K_{trans}). ROIs are demarcated in MA (**a, d**), MP (**b, e**), and LP (**c, f**) muscle pairs. (For interpretation of the references to colour in this figure legend, the reader is referred to the Web version of this article.)

Table 2 Interrater reliability expressed as ICC coefficient (95 % confidence interval).

Muscle	Side	K_{trans}	k_{ep}	v_e	v_p
Lateral pterygoid	Left	0.97 (0.953, 0.981)	0.973 (0.957, 0.983)	0.979 (0.968, 0.987)	0.992 (0.987, 0.995)
	Right	0.988 (0.981, 0.992)	0.985 (0.977, 0.99)	0.943 (0.912, 0.964)	0.986 (0.979, 0.991)
Masseter	Left	0.901 (0.845, 0.936)	0.913 (0.864, 0.944)	0.995 (0.992, 0.997)	0.997 (0.995, 0.998)
	Right	0.99 (0.985, 0.994)	0.993 (0.99, 0.996)	0.974 (0.959, 0.983)	0.999 (0.998, 0.999)
Medial pterygoid	Left	0.983 (0.973, 0.989)	0.99 (0.984, 0.993)	0.942 (0.909, 0.963)	0.989 (0.983, 0.993)
	Right	0.985 (0.977, 0.99)	0.987 (0.979, 0.992)	0.975 (0.961, 0.984)	0.995 (0.992, 0.997)

K_{trans}: transfer constant between blood plasma and the extravascular extracellular space (min^{-1}).
k_{ep}: rate constant between the extravascular extracellular space and blood plasma (min^{-1}).
v_e: volume of the extravascular extracellular space per unit volume of tissue (%).
v_p: blood plasma per unit volume of tissue (%).

Table 3 Medians (interquartile ranges) of quantitative DCE MRI biomarkers in each muscle group.

Muscle	Condyle Grade	K_{trans} (1/min/1000)	*P*-value	k_{ep} (1/min/1000)	*P*-value	v_e (1/1000)	*P*-value	v_p (1/1000)	*P*-value
Lateral pterygoid	0	163.4 (146.9)	0.122	1158.1 (943.6)	0.179	191.6 (130.9)	0.863	26.1 (61.1)	0.032*
	1	204.3 (147.5)		1427.5 (1012.6)		178.2 (126.9)		40.1 (55.9)	
	2	167.2 (151.7)		1119 (872)		199.8 (150.1)		58.2 (103.9)	
Masseter	0	149.5 (103.2)	0.277	1095.2 (600.2)	0.092	147.9 (66.8)	0.330	38.6 (66.1)	0.356
	1	156.5 (108.2)		1076.3 (752.4)		151.9 (65.1)		32.6 (60.8)	
	2	140.6 (94.3)		900.7 (621.2)		166.1 (97.7)		51.9 (80.1)	
Medial pterygoid	0	149.7 (83.9)	0.170	1246.6 (670.1)	0.256	132.4 (72.2)	0.989	35.7 (44.8)	0.349
	1	157.9 (72.5)		1389.2 (637.6)		132.1 (47)		43.8 (45.1)	
	2	141.4 (92.2)		1224.3 (627.2)		140.2 (58.4)		51.6 (76.3)	

*Kruskal—Wallis test (*P*-value <0.05).
K_{trans}: transfer constant between blood plasma and the extravascular extracellular space (min^{-1}).
k_{ep}: rate constant between the extravascular extracellular space and blood plasma (min^{-1}).
v_e: volume of the extravascular extracellular space per unit volume of tissue (%).
v_p: blood plasma per unit volume of tissue (%).

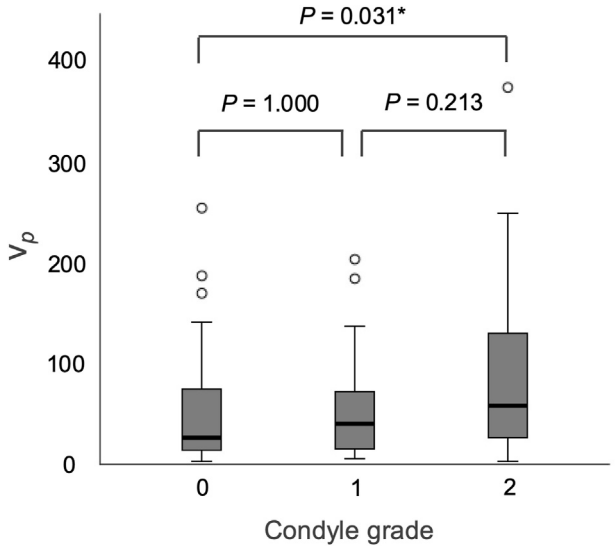

Figure 4 Medians of blood plasma per unit volume of tissue (v_p) with DCE MRI values across different condyle grades in LP muscle. Pairwise comparisons with Kruskal–Wallis test adjusted using Bonferroni's correction: condyle grade 0 versus grade 1 ($P = 1.000$), condyle grade 0 versus grade 2 ($P = 0.031$), and condyle grade 1 versus grade 2 ($P = 0.213$).

normal condyle (grade 0). However, no significant differences of v_p values were found in the MA or MP muscles. Similarly, changes in the vascular permeability parameters (K_{trans} and k_{ep}) were not significant in the MA, MP, or LP muscles. Additionally, the unique anatomical attachment of the LP muscle to the TMJ capsule suggests a potential correlation between increased LP muscle perfusion and bony condylar resorption.

The LP muscle plays a pivotal role in mastication and is implicated in the pathophysiology of TMDs. Morphological changes in the LP muscle, such as muscle hypertrophy, are observable on MRI and are associated with various TMD manifestations, including anterior disk displacement without reduction, condylar arthrosis and joint effusion.[18,19] Hypertrophy of the LP muscle correlates with painful TMDs accompanied by migraines.[20] These findings suggest a compensatory response to mechanical overload or hyperactivity within the masticatory system.[21,22] By contrast, muscle atrophy often accompanies degenerative TMJ conditions[23] and follows procedures such as artificial TMJ replacement,[24] suggesting muscle detachment and subsequent functional impairment. In an animal model, Lemos et al.[25] discovered that TMJ arthritis reduced the area and diameter of masticatory muscle fibers, particularly in the LP muscle. They reported a unique anatomical and functional aspect in the LP muscle as the only masticatory muscle that directly inserts into the TMJ.

Several studies have used MRI to examine signal changes within the LP muscle in patients with TMDs. For instance, Kuroda et al.[26] used fluid-attenuated inversion recovery images of the LP muscle and reported a positive correlation between signal intensity ratio and pain score. Soydan et al.[27] identified a correlation between signal intensity ratio on T1-and T2-weighted images and the extent of disk displacement. Similar findings were reported by Yesiltepe et al.,[19] who observed a higher signal intensity in proton density images of the superior LP muscle in patients with anterior disk displacement without reduction compared with those with reduction. These morphological and muscle signal changes emphasize the clinical importance of the LP muscle, reflecting its anatomical connectivity to the condyle, disk, and glenoid cavity and its pivotal role in TMD-associated pain. These findings confirm the distinctive role of the LP muscle in TMD pathology and provide quantifiable insights into the disease's morphological manifestations. They also confirm the presence of increased perfusion in the LP muscle in patients with ICR.

We also observed a considerable increase in plasma volume in the LP muscle in patients with severe condylar resorption (grade 2) of the TMJ. This pattern was not observed in the MA or MP muscles. Being anatomically distinct, the LP muscle is the only masticatory muscle that directly inserts into the mandibular condyle.[28–30] This unique relationship indicates that the observed increase in plasma volume may be a consequence of bone–muscle interactions. Although studies on TMDs and ICR have primarily focused on intrajoint dynamics,[3,6,31,32] particularly the relationship between discs and joints, the complex interplay between musculature and jawbone changes has not been comprehensively examined. In a study on muscle–bone interactions, Ishizuka et al.[33] reported a direct correlation between muscle deformation and bone volume with the progression of TMJ osteoarthritis in a mouse model. This correlation was evidenced by an increase in temporal muscle deformation positively correlating with mandibular head volume and a negative correlation with retromandibular connective tissue. Xu et al.[34] examined how musculature alterations affect subchondral bones and discovered that subchondral bone changes and cartilage degeneration occurred as results of quadriceps muscle atrophy in osteoarthritic rats. Similarly, Moverman et al.[35] reported a correlation between rotator cuff muscle atrophy and glenoid bone deformity in shoulder osteoarthritis. These findings are consistent with ours, emphasizing the key role of muscle–bone interactions, particularly augmented perfusion in the LP muscle and condylar resorption, in understanding the mechanisms underlying TMDs and ICR.

In DCE MRI examinations, plasma volume is commonly regarded as an indicator of microvascular density.[36] Elevated inflammation levels stimulate bone resorption.[37] In an animal study involving DCE MRI, Qi et al.[38] examined denervated skeletal muscles and discovered an increase in K_{trans} and v_p values in these muscles. This increase occurred before electromyography abnormalities and conventional MRI signal intensity changes. These findings indicate that DCE MRI has the potential to serve as an early and sensitive diagnostic tool. Overall, these studies and concepts corroborate our findings, indicating the crucial role of muscle–bone interactions in patients with ICR and TMDs.

Multiple studies have focused on treatments targeting the LP muscle in patients with TMDs. For instance, in a randomized clinical study, Rezazadeh et al.[39] examined the effects of botulinum toxin A injection on the LP muscle in patients with painful TMDs. In a randomized controlled trial, Olbort et al.[40] explored the efficacy of LP muscle training for patients with painful TMDs. Overall, our study

provides valuable insights into potential treatments for TMDs, specifically focusing on LP muscle changes in DCE MRI biomarkers.

This study has several limitations. First, we predominantly focused on masticatory muscles and their connection with condylar resorption in patients with ICR. ICR is a multifaceted condition that involves various anatomical structures, including bone, muscle, TMJ disks, and retrodiscal tissues, and the coordination of adjacent anatomical elements. Our exclusive focus on masticatory muscles may limit the overall understanding of the broader muscular and skeletal alterations in ICR and TMDs. Second, DCE MRI parameters may yield different results with various post-processing models, image acquisition protocols, and potential confounding variables, such as patient movement and imaging artifacts. These elements may limit the generalizability and clinical applicability of our findings. In this study, we used the quantitative Tofts model to provide universally consistent data on vascular kinetics and increase the popularity of DCE MRI among different users. Third, this study lacked data on additional potential contributing clinical factors, such as joint loading patterns, occlusal parameters, and inflammatory processes. Future research should include these clinical factors to achieve more comprehensive results. Fourth, our sample size was relatively moderate. A larger sample size would enable a more robust analysis and a deeper exploration of the relationship between muscles and bones within the TMJ. Fifth, our study was cross-sectional in nature, which inherently prevented establishing a causal relationship between muscle perfusion alterations and condylar resorption. Longitudinal studies with follow-up assessments are required to obtain valuable insights into the temporal dynamics and progression of these changes.

This study established a link between increased microcirculation in the LP muscle and TMJ condylar resorption severity in patients with ICR. It also provides valuable insights into the interactions between masticatory muscles and condylar resorption in patients with ICR and the efficacy of utilizing DCE MRI in TMD evaluations. Overall, our findings lay the foundation for future research seeking to develop therapeutic approaches for patients with TMDs and ICR.

Declaration of competing interest

The authors have no conflicts of interest relevant to this article.

Acknowledgments

This study was supported by the Ministry of Science and Technology, Taiwan (MOST, 107-2314-B-002-103-MY3).

References

1. Peck CC, Goulet JP, Lobbezoo F, et al. Expanding the taxonomy of the diagnostic criteria for temporomandibular disorders. *J Oral Rehabil* 2014;41:2—23.
2. Schiffman E, Ohrbach R, Truelove E, et al. Diagnostic Criteria for Temporomandibular Disorders (DC/TMD) for clinical and research applications: recommendations of the international RDC/TMD consortium network* and orofacial pain special interest group†. *J Oral Facial Pain Headache* 2014;28:6—27.
3. Mitsimponas K, Mehmet S, Kennedy R, Shakib K. Idiopathic condylar resorption. *Br J Oral Maxillofac Surg* 2018;56:249—55.
4. Posnick JC, Fantuzzo JJ. Idiopathic condylar resorption: current clinical perspectives. *J Oral Maxillofac Surg* 2007;65:1617—23.
5. Arnett GW, Gunson MJ. Risk factors in the initiation of condylar resorption. *Semin Orthod* 2013;19:81—8.
6. Mercuri LG, Handelman CS. Idiopathic condylar resorption: what should we do? *Oral Maxillofac Surg Clin* 2020;32:105—16.
7. Abramowicz S, Kim S, Prahalad S, Chouinard AF, Kaban LB. Juvenile arthritis: current concepts in terminology, etiopathogenesis, diagnosis, and management. *Int J Oral Maxillofac Surg* 2016;45:801—12.
8. Larheim TA, Abrahamsson AK, Kristensen M, Arvidsson LZ. Temporomandibular joint diagnostics using CBCT. *Dentomaxillofacial Radiol* 2015;44:20140235.
9. Xiong X, Ye Z, Tang H, et al. MRI of temporomandibular joint disorders: recent advances and future directions. *J Magn Reson Imag* 2021;54:1039—52.
10. Arslan A, Orhan K, Paksoy CS, et al. MRI evaluation of the classification, frequency, and disc morphology of temporomandibular joint disc displacements: a multicenter retrospective study in a Turkish population. *Oral Radiol* 2009;25:14—21.
11. Ma GMY, Calabrese CE, Donohue T, et al. Imaging of the temporomandibular joint in juvenile idiopathic arthritis: how does quantitative compare to semiquantitative MRI scoring? *J Oral Maxillofac Surg* 2019;77:951—8.
12. Buch K, Peacock ZS, Resnick CM, Rothermel H, Kaban LB, Caruso P. Regional differences in temporomandibular joint inflammation in patients with juvenile idiopathic arthritis: a dynamic post-contrast magnetic resonance imaging study. *Int J Oral Maxillofac Surg* 2020;49:1210—6.
13. Caruso P, Buch K, Rincon S, et al. Optimization of quantitative dynamic postgadolinium MRI technique using normalized ratios for the evaluation of temporomandibular joint synovitis in patients with juvenile idiopathic arthritis. *AJNR Am J Neuroradiol* 2017;38:2344—50.
14. Tasali N, Cubuk R, Aricak M, et al. Temporomandibular joint (TMJ) pain revisited with dynamic contrast-enhanced magnetic resonance imaging (DCE-MRI). *Eur J Radiol* 2012;81:603—8.
15. Stoustrup PB, Ahlefeldt-Laurvig-Lehn N, Kristensen KD, et al. No association between types of unilateral mandibular condylar abnormalities and facial asymmetry in orthopedic-treated patients with juvenile idiopathic arthritis. *Am J Orthod Dentofacial Orthop* 2018;153:214—23.
16. Kellenberger CJ, Junhasavasdikul T, Tolend M, Doria AS. Temporomandibular joint atlas for detection and grading of juvenile idiopathic arthritis involvement by magnetic resonance imaging. *Pediatr Radiol* 2018;48:411—26.
17. Tofts PS, Brix G, Buckley DL, et al. Estimating kinetic parameters from dynamic contrast-enhanced t_1-weighted MRI of a diffusable tracer: standardized quantities and symbols. *J Magn Reson Imag* 1999;10:223—32.
18. Taşkaya-Yýlmaz N, Oğütcen-Toller M. Clinical correlation of MRI findings of internal derangements of the temporomandibular joints. *Br J Oral Maxillofac Surg* 2002;40:317—21.
19. Yesiltepe S, Kılcı G, Gök M. Evaluation of the lateral pterygoid muscle area, attachment type, signal intensity and presence of arthrosis, effusion in the TMJ according to the position of the articular disc. *J Stomatol Oral Maxillofac Surg* 2022;123:e973—80.
20. Lopes SLP de C, Costa ALF, Gamba T de O, Flores IL, Cruz AD, Min LL. Lateral pterygoid muscle volume and migraine in patients with temporomandibular disorders. *Imaging Sci Dent* 2015;45:1—5.

21. D'Ippolito SM, Borri Wolosker AM, D'Ippolito G, Herbert de Souza B, Fenyo-Pereira M. Evaluation of the lateral pterygoid muscle using magnetic resonance imaging. *Dentomaxillofacial Radiol* 2010;39:494—500.
22. Yang X, Pernu H, Pyhtinen J, Tiilikainen PA, Oikarinen KS, Raustia AM. MR abnormalities of the lateral pterygoid muscle in patients with nonreducing disk displacement of the TMJ. *Cranio* 2002;20:209—21.
23. Taskaya-Yilmaz N, Ceylan G, Incesu L, Muglali M. A possible etiology of the internal derangement of the temporomandibular joint based on the MRI observations of the lateral pterygoid muscle. *Surg Radiol Anat* 2005;27:19—24.
24. Zhong YQ, Sun Q, He DM, Zou LX, Lu C. Study on the lateral pterygoid muscle status after artificial temporomandibular joint replacement. *Int J Oral Maxillofac Surg* 2021;50:1496—501.
25. Lemos GA, da Silva PLP, Batista AUD, Palomari ET. Experimental model of temporomandibular joint arthritis: evaluation of contralateral joint and masticatory muscles. *Arch Oral Biol* 2018;95:79—88.
26. Kuroda M, Otonari-Yamamoto M, Araki K. Evaluation of lateral pterygoid muscles in painful temporomandibular joints by signal intensity on fluid-attenuated inversion recovery images. *Oral Radiol* 2018;34:17—23.
27. Soydan Çabuk D, Etöz M, Akgün İE, Doğan S, Öztürk E, Coşgunarslan A. The evaluation of lateral pterygoid signal intensity changes related to temporomandibular joint anterior disc displacement. *Oral Radiol* 2021;37:74—9.
28. Carpentier P, Yung JP, Marguelles-Bonnet R, Meunissier M. Insertions of the lateral pterygoid muscle: an anatomic study of the human temporomandibular joint. *J Oral Maxillofac Surg* 1988;46:477—82.
29. Murray GM, Phanachet I, Uchida S, Whittle T. The human lateral pterygoid muscle: a review of some experimental aspects and possible clinical relevance. *Aust Dent J* 2004;49:2—8.
30. Murray GM, Bhutada M, Peck CC, Phanachet I, Sae-Lee D, Whittle T. The human lateral pterygoid muscle. *Arch Oral Biol* 2007;52:377—80.
31. Alsabban L, Amarista FJ, Mercuri LG, Perez D. Idiopathic condylar resorption: a survey and review of the literature. *J Oral Maxillofac Surg* 2018;76:2316.e1—2316.e13.
32. Shen P, Zhang D, Luo Y, Abdelrehem A, Yang C. Characteristics of patients with temporomandibular joint idiopathic condylar resorption. *Cranio* 2022;43:1—7.
33. Ishizuka S, Yamamoto M, Hirouchi H, et al. Muscle-bone relationship in temporomandibular joint disorders after partial discectomy. *J Oral Biosci* 2021;63:436—43.
34. Xu J, She G, Gui T, et al. Knee muscle atrophy is a risk factor for development of knee osteoarthritis in a rat model. *J Orthop Translat* 2020;22:67—72.
35. Moverman MA, Puzzitiello RN, Menendez ME, et al. Rotator cuff fatty infiltration and muscle atrophy: relation to glenoid deformity in primary glenohumeral osteoarthritis. *J Shoulder Elb Surg* 2022;31:286—93.
36. Keil VC, Pintea B, Gielen GH, et al. Meningioma assessment: kinetic parameters in dynamic contrast-enhanced MRI appear independent from microvascular anatomy and VEGF expression. *J Neuroradiol* 2018;45:242—8.
37. Epsley S, Tadros S, Farid A, Kargilis D, Mehta S, Rajapakse CS. The effect of inflammation on bone. *Front Physiol* 2020;11:511799.
38. Qi L, Xu L, Wang WT, et al. Dynamic contrast-enhanced magnetic resonance imaging in denervated skeletal muscle: experimental study in rabbits. *PLoS One* 2019;14:e0215069.
39. Rezazadeh F, Esnaashari N, Azad A, Emad S. The effects of botulinum toxin A injection on the lateral pterygoid muscle in patients with a painful temporomandibular joint click: a randomized clinical trial study. *BMC Oral Health* 2022;22:217.
40. Olbort C, Pfanne F, Schwahn C, Bernhardt O. Training of the lateral pterygoid muscle in the treatment of temporomandibular joint disc displacement with reduction: a randomised clinical trial. *J Oral Rehabil* 2023;50:921—30.